

Electronic structure of palladium (100)

J. G. Gay, J. R. Smith, F. J. Arlinghaus, and T. W. Capehart

Physics Department, General Motors Research Laboratories, Warren, Michigan 48090

(Received 21 August 1980)

The electronic structure of palladium (100) is calculated using the self-consistent local orbital method. A work function of 5.0 eV is obtained. A large density of surface states is found that approaches the density found for Ni(100). A new method of displaying the electronic structure is introduced in which the densities of states in a number of small regions of the two-dimensional Brillouin zone are calculated. Plots of these \vec{k}_{\parallel} -selected densities of states (DOS) are given for \vec{k}_{\parallel} vectors spanning the $\bar{\Gamma}$ - \bar{X} (110) and $\bar{\Gamma}$ - \bar{M} (100) directions. The \vec{k}_{\parallel} -selected DOS of the even mirror plane symmetry states were found to be quite different from those of the odd-symmetry states. This gives added importance to the use of polarized light in photoemission. These \vec{k}_{\parallel} -selected DOS vary rapidly with \vec{k}_{\parallel} and with location relative to the surface. There are peaks in the surface plane projection which correspond to surface states. Hopefully the plots will facilitate the experimental identification of surface-state bands in metals.

I. INTRODUCTION

We have previously used our self-consistent local orbital (SCLO) method¹ to compute the surface electronic structure of Cu(100) (Refs. 1 and 2) and Ni(100) (Ref. 3). For Cu(100) (Refs. 1 and 2) we found a large surface-state-surface-resonance density located near the top of the d band which we used to explain the large attenuation in photoemission signal near the top of the d band in chemisorption experiments on Cu(100) (Refs. 4 and 5). This density includes an unambiguous surface-state band lying above the bulk d bands at the \bar{M} point in the two-dimensional Brillouin zone. The presence of this band was subsequently observed experimentally.⁶ The high surface-state density is apparently the consequence of a subtlety in the self-consistent Cu(100) potential since earlier non-self-consistent but otherwise sophisticated Cu(100) calculations⁷⁻⁹ predict no significant surface-state density at the top of the d band.

In the entirely analogous calculation on paramagnetic Ni(100) (Ref. 3) we found somewhat fewer surface states which further were not concentrated in any energy interval. This led us to speculate that this difference might be due to the effect of the filled Cu(100) surface states themselves on the self-consistent potential which is absent in the Ni(100) potential.

Louie¹⁰ has shown, for Pd(111), that a substantial surface-state density exists in a region centered about 1 eV below the Fermi level and has suggested it is responsible for a decrease in photoemission signal at that energy in chemisorption experiments.¹¹ Decreases have been observed in chemisorption of CO and C₆H₆ on Pd(100).¹²

In an attempt to further our understanding of transition-metal surface-state properties we have computed the electronic structure of Pd(100) and report the results here. In Sec. II we describe the

application of the SCLO method to Pd(100) and present the surface electronic structure in the form of the two-dimensional band structure with surface states delineated, as well as planar and total densities of states. In Sec. III we analyze the electronic structure in a new fashion by computing densities of states arising from states located in a number of small regions of the two-dimensional Brillouin zone. These \vec{k}_{\parallel} -selected densities of states may be useful in locating surface-state bands with angle-resolved photoemission experiments. Our results are summarized in Sec. IV.

II. Pd(100) ELECTRONIC STRUCTURE

The SCLO method, as applied to Cu(100), has been described in detail.¹ The only changes required for Pd(100) are related to the additional number and complexity of the atomic orbitals of a $4d$ metal as compared with a $3d$ metal. In fitting the atomic orbitals of palladium we used 13 s -type, 9 p -type, and 7 d -type Gaussian orbitals: two more of each angular momentum type than for copper. The $5p$, $5d$, and $6s$ orbitals were constructed exactly as the $4p$, $4d$, and $5s$ orbitals were for copper. The atomic-potential fits used 16 instead of 14 Gaussians. In the atomic calculation upon which these fits were based we used a $4d^{9.5}5s^{0.5}$ configuration. In other respects the calculation is analogous to the copper and nickel calculations. The same number of components is used in the Fourier transform and the mesh size used in computing transforms of the charge density was again chosen to be $\frac{1}{10}$ of the lattice constant. The iteration to self-consistency was carried out using 3 \vec{k}_{\parallel} points in the irreducible part of the Brillouin zone. The Wigner interpolation formula was used for the exchange correlation potential.

For Cu(100) and Ni(100) we used a nine-plane slab to insure a slab sufficiently thick to study

surface states. However, comparison of seven- and nine-plane results for Cu(100) has convinced us that seven planes give essentially the same surface-state density as nine planes. Accordingly, as a matter of economy, we have chosen to limit the Pd(100) slab to seven planes. We initiated the 7-plane calculation by carrying out a three-plane calculation. The self-consistent charge density for this calculation was used, as described in Ref. 1, to generate a starting charge density for the seven-plane slab which was then iterated to self-consistency.

After the self-consistent solution has been determined, the electronic structure of the slab is computed at 45 uniformly spaced points in the elementary $\frac{1}{8}$ of the surface Brillouin zone. These solutions are used to compute electronic densities of states and to display the energy bands of the slab.

Densities of states (DOS) for palladium are shown in Fig. 1. In general shape and width our

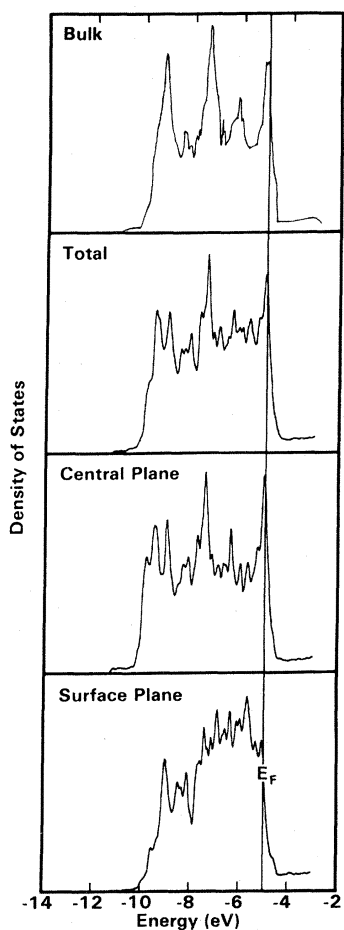


FIG. 1. Density-of-states curves for the seven-plane Pd(100) film. The bulk density of states was taken from Ref. 13.

planar¹ DOS for the central plane and our total DOS for the seven-plane slab agree well with the bulk density of states of palladium computed by Moruzzi, Janak, and Williams.¹³ Both should converge, in the limit of a large number of planes, to the bulk DOS which would result from using our basis set in a bulk calculation. On the other hand, the surface-plane DOS is distinctly narrower and, compared to the bulk, has a higher density about 1 V below E_F . The narrowing is expected because the surface atoms have fewer neighbors. The higher density is a result of surface states as we now describe.

The operational definition which we used to distinguish surface states in the nine-plane Cu and Ni calculations was that at least 80% of their charge must reside in the outer two planes of the slab. We retain this definition here but recognize that it is a different, and less stringent, criterion for a 7-plane slab. If we number the surface plane of the slab 1, the next plane beneath it 2, etc., the definition is

$$[\rho(1) + \rho(2)] / [\frac{1}{2}\rho(4) + \rho(3) + \rho(2) + \rho(1)] \geq 80\%, \quad (1)$$

where $\rho(i)$ is the surface-state charge in layer i .

This criterion can be applied to a slab of any number of planes greater than or equal to seven and will give results independent of thickness for sufficiently thick slabs. The definition obviously encompasses both surface states and strong resonances but, for convenience in discussion, states meeting the criterion will henceforth be termed simply surface states.

Figure 2 shows the two-dimensional band structure of the slab along high-symmetry directions in the Brillouin zone. Surface states are indicated by open circles. There is a definite concentration of these states in a region centered about -6 eV, though the concentration is not so pronounced as the concentration of surface states at the top of the d band in Cu(100). Nevertheless, the surface states contribute approximately $\frac{1}{3}$ of the DOS in the surface plane in this region of energy and in fact 19% of the surface plane charge (1.9 electrons per surface atom) is contributed by surface states. This is to be compared with 36% for Cu(100) and 23% for Ni(100) (4.0 and 2.3 electrons per surface atom, respectively).

Bulk-band projections along the directions $\bar{\Gamma}-\bar{X}$ and $\bar{\Gamma}-\bar{M}$ show¹⁴ a single narrow absolute gap below E_F starting about halfway from $\bar{\Gamma}$ to \bar{X} and running to \bar{X} . The gap starts at about -9 V on Fig. 2 and rises to about -8.5 V at \bar{X} . The region of low density at about -9 V at \bar{X} in Fig. 2 may be an indication of this gap. The sparsity of absolute gaps within the d band displayed by these projections suggests that there are few true surface states

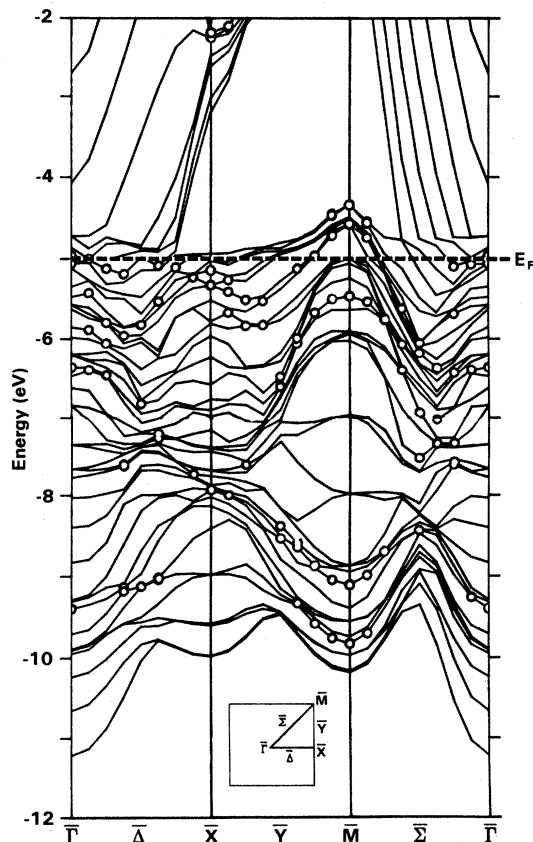


FIG. 2. Surface band structure along high-symmetry directions for the seven-plane Pd(100) slab. The open circles represent states on the $45 \vec{k}_\parallel$ -point mesh (see text) which are highly localized in the surface plane of the slab.

on Pd(100) there. Another, much larger absolute gap is found around \bar{M} and runs in Fig. 2 along \bar{Y} above the top of the d band (above -5 eV). Some of the circled states in Fig. 2 above the Fermi level near \bar{M} lie in this gap.

We have tested the thickness dependence of the criterion [Eq. (1)] for Cu(100) for which we have solutions for seven and nine planes. We find that 34.8% of the surface plane charge is contributed by surface states for seven planes while we find 35.8% for nine planes. Comparison of the seven- and nine-plane band structures shows almost identical surface-state bands. Thus our criterion for surface states appears essentially independent of thickness beyond seven planes.

The selection of 80% in (1) is arbitrary. To see if the ordering of the three metals according to the fraction of surface-layer electrons in surface states is independent of this percentage, we have computed surface-state fractions for 75%, 85%, and 90%. The results plotted in Fig. 3 show

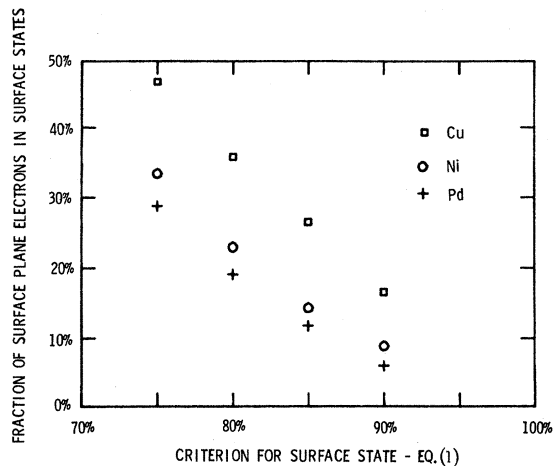


FIG. 3. Dependence of the surface-state contribution to the surface plane charge density on the degree of surface localization required for acceptance as a surface state.

that the ordering is independent of the percentage chosen. The 80% criterion does select highly localized surface states. The surface plane and the second plane in from the surface contain 52% and 32% of the surface-state electronic charge while the next two planes in from the surface account for only 9% and 7%, respectively.

There is, to our knowledge, only one measurement of the work function of Pd(100). A value of 5.3 eV has been found by Bradshaw.¹⁵ Our theoretical value of 5.0 eV is in reasonable agreement with that experimental number. While 0.3 eV is the largest disagreement with experiment we have had for the electron work function, it is perhaps within our error bar. We do note that relativistic corrections may not be negligible in Pd (Ref. 16) and will likely act to increase the work function.

III. \vec{k}_\parallel -SELECTED DENSITIES OF STATES

There has been much activity in the last five years in angular photoemission studies from solid surfaces. The relationship between angular photoemission spectra and the electronic structure of the solid can be quite complex.¹⁷⁻²³

In the simplest picture, the photoemission intensity is given by a modulation of an initial density of states, a final density of states, an optical transition probability, and an escape factor representing the probability of the excited electron reaching the surface without inelastic scattering and then escaping across it. The escape factor is usually treated as a constant. The optical transition probability is often also taken to be constant, although it has been computed using free-electron final states or using atomiclike dipole selection rules.²³

Two distinct approaches have evolved to treat the initial- and final-state components of the photoemission intensity. In the direct-transition model, optical transitions are allowed only if

$$\vec{k}_f = \vec{k}_i + \vec{G}, \quad (2)$$

where \vec{k}_f is the Bloch vector of the final state, k_i that of the initial state, and \vec{G} is a reciprocal-lattice vector. Equation (2) would be valid if the photoexcitation process occurs in the bulk of the crystal. Peak positions are often given well by the direct-transition model using bulk electronic structures and free-electron final states²³ indicating that significant information concerning bulk electronic structure is available from angular photoemission data.

The second approach assumes that the excitation occurs in the surface region of the crystal and that only the parallel component k_{\parallel} of \vec{k} is conserved since in the vicinity of the surface the perpendicular component k_{\perp} is not conserved. If one relaxes the conservation of k_{\perp} completely and takes the optical transition probability and escape factor to be constants, then the photoemission intensity is given by the one-dimensional density of initial states for the appropriate k_{\parallel} . This quantity has been calculated in the past using only *bulk* band-structure results and for a single k_{\parallel} .^{23, 24}

One can relax the conservation of k_{\perp} partially by employing, for example, a Lorentzian broadening function $L(k_{\perp}, k_{\perp i})$ of the form

$$L(k_{\perp}, k_{\perp i}) = [\gamma^2 + (k_{\perp}^2 - k_{\perp i}^2)]^{-1} \quad (3)$$

in the joint modulation of initial and final states. Sugarton and Shevchik²³ have shown for one theoretical spectrum from Cu(111) that when $\gamma > 0.5$ eV the computed energy distribution curve is very similar to the one-dimensional density of states, as might be expected.

It is clear if one is interested in photoemission from states localized in the surface region, then the second approach is the more appropriate since k_{\perp} is not a good quantum number for these states. This is borne out experimentally, for example, in the successful mapping out of the two-dimensional surface-state band on Cu(100) by Heimann *et al.*⁶ Another example where k_{\perp} is not conserved is adsorbate band structure which can now be probed via angular photoemission experiments.¹⁴

Since the Pd(100) surface electronic structure has a high concentration of states localized in the surface region, we have elected to analyze it by an extension of the one-dimensional density-of-states approach. As described in Ref. 1, the starting point for the conventional DOS calculations (Fig. 1) is a set of solutions to the final self-consistent potential at 45 regularly spaced points in the ir-

reducible part of the two-dimensional Brillouin zone. These are used in conjunction with an interpolation scheme to generate approximate solutions at a large number of randomly selected points in the zone. Here, instead of selecting the points throughout the whole zone, they are randomly selected within a small square centered about a specified k_{\parallel} . The result we call k_{\parallel} -selected densities of states.

We have calculated k_{\parallel} -selected densities along the high-symmetry directions $\bar{\Gamma}$ to \bar{X} and $\bar{\Gamma}$ to \bar{M} using the scheme depicted in Fig. 4. The squares are $\pi/5a$ on a side where a is the surface lattice constant and 1000 points were interpolated in each square. The squares are labeled $\frac{1}{4}$, $\frac{1}{2}$, etc., to indicate their position on the $\bar{\Gamma}$ - \bar{X} or $\bar{\Gamma}$ - \bar{M} lines. For Pd, $\pi/5a = 0.23 \text{ \AA}^{-1}$. This width was selected to simulate the angular resolution of $\pm 2^\circ$, which is representative of analyzers presently employed in photoemission experiments. The experimental error in determining k_{\parallel} due to finite angular resolution increases with increasing photon energy E_p and with decreasing angle of emission θ relative to the surface normal as can be seen from Eq. (5) below. For $\theta = 0$, $E_p = 40.8$ eV, and $\Delta\theta = \pm 2^\circ$, the uncertainty in $|k_{\parallel}|$ is $\sim 0.2 \text{ \AA}^{-1}$, which is comparable to our chosen box width.

For the high-symmetry lines $\bar{\Gamma}$ - \bar{X} and $\bar{\Gamma}$ - \bar{M} which pass through the origin ($\bar{\Gamma}$) Hermanson²⁵ has argued that the one-electron final state is invariant under reflection through those lines because the surface component of the momentum is unchanged. Thus since transition probability

$$\propto |\langle f | \vec{A} \cdot \vec{r} | i \rangle|^2, \quad (4)$$

the symmetry of an allowed initial state $|i\rangle$ must be the same as $\vec{A} \cdot \vec{r}$, where \vec{A} is the

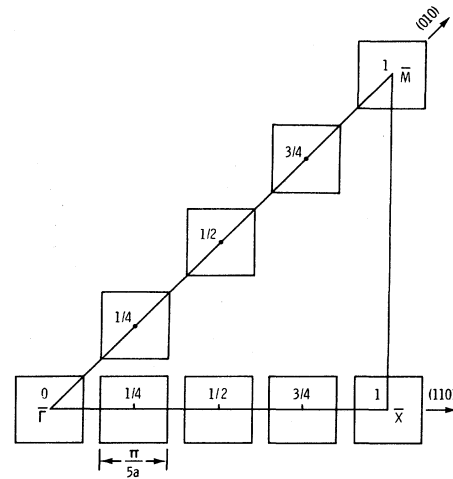


FIG. 4. Regions of k_{\parallel} space selected for density-of-states computations.

(spatially constant) vector potential. Hence by varying the light polarization one can select states which are either *even* or *odd* with respect to reflection across the symmetry line (mirror plane). Therefore we compute the even and odd components of the \vec{k}_{\parallel} -selected DOS. Experimental data are typically reported as photoelectron emission intensity versus electron kinetic energy (energy distribution curve or EDC) at a given angle of emission θ relative to the surface normal. One can use these data to make initial-state electronic eigenvalue E_I vs \vec{k}_{\parallel} plots, which may be compared with surface-state bands such as those shown in Fig. 2. Alternatively, one may compare surface-state peak shapes in our \vec{k}_{\parallel} -selected DOS with peak shapes in an EDC. In addition to problems with energy-dependent cross sections and final-state effects, there is the complication that at a given θ , $|\vec{k}_{\parallel}|$ varies as E_I varies,

$$|\vec{k}_{\parallel}| = [2(E_v - E_I)]^{1/2} \sin \theta, \quad (5)$$

where E_v is the photon energy. One can see that this variation of $|\vec{k}_{\parallel}|$ decreases with increasing E_v and decreasing θ . One can quantitatively assess this for $E_v = 40.8$ eV and θ such that the middle of the Pd(100) d band is at $|\vec{k}_{\parallel}| = \pi/a$ (zone boundary along $\bar{\Gamma} - \bar{X}$). Then the variation of $|\vec{k}_{\parallel}|$ over the d -band width (5 eV variation of E_I) is $\pi/100$. Thus the variation of \vec{k}_{\parallel} with E_I at a given collection angle θ does not appear to be a problem for 40.8-eV photon energies.

To spell out the method of separation into even and odd states under reflection we recall from Ref. 1 that an SCLO eigenfunction $\psi_i(\vec{k}_{\parallel}, \vec{r})$, belonging to a wave vector \vec{k}_{\parallel} , is a linear combination of slab Bloch functions

$$\psi_i(\vec{k}_{\parallel}, \vec{r}) = \sum_{j=1}^M U_{ij}(\vec{k}_{\parallel}) \phi_j(\vec{k}_{\parallel}, \vec{r}), \quad (6)$$

which are, in turn, linear combinations of the local orbitals

$$\phi_j(\vec{k}_{\parallel}, \vec{r}) = N^{-1/2} \sum_{\vec{n}} e^{i\vec{k}_{\parallel} \cdot \vec{n}} a_j(\vec{r} - \vec{n}). \quad (7)$$

The index j is a compound index which gives both the orbital type and the plane in which it is located, and the vector \vec{n} runs over the atom positions of plane j in the N unit cells of the slab. Corresponding to each orbital type $a_j(\vec{r})$ in each plane there is a projected DOS $n_j(E)^2$. The contribution of $\psi_i(\vec{k}_{\parallel}, \vec{r})$ at its energy E to $n_j(E)$ is

$$U_{ij}(\vec{k}_{\parallel}) \sum_{i=1}^M S_{ij}(\vec{k}_{\parallel}) U_{ii}(\vec{k}_{\parallel}). \quad (8)$$

To obtain the even and odd DOS along $\bar{\Gamma} - \bar{X}$ these quantities are interpolated and those corresponding to orbitals even under reflection are added to

obtain the even DOS, and similarly for the odd DOS. Since some of the basic SCLO orbitals happen not to be even or odd under a reflection in the plane containing the $\bar{\Gamma} - \bar{M}$ direction, new orbitals, which are simple linear combinations of the basic orbitals, are constructed and quantities corresponding to (8) are interpolated to obtain the even and odd DOS along $\bar{\Gamma} - \bar{M}$.

The above procedure is not precisely correct since it presumes the $\phi_j(\vec{k}_{\parallel}, \vec{r})$ are entirely even or odd. This is not true when \vec{k}_{\parallel} lies out of the mirror plane. For example, for \vec{k}_{\parallel} lying near the $\bar{\Gamma} - \bar{X}$ plane, with components k_x along $\bar{\Gamma} - \bar{X}$ and a small component k_y , we have

$$\phi_j(\vec{k}_{\parallel}, \vec{r}) \simeq \phi_j(k_x, \vec{r}) + ik_y \sum_{\vec{n}} n_y e^{i\vec{k}_x \cdot \vec{n}} a_j(\vec{r} - \vec{n}) \quad (9)$$

where, because the $a_j(\vec{r} - \vec{n})$ are localized, the \vec{n} 's which contribute to (9) are not large. While $\phi_j(k_x, \vec{r})$ is pure even or odd, we see that there is in addition a small term in (9) of opposite parity which is of order k_y . Similarly,

$$S_{ij}(\vec{k}_{\parallel}) \simeq S_{ij}(\vec{k}_x) + ik_y \sum_{\vec{n}} n_y e^{i\vec{k}_x \cdot \vec{n}} \int a_i(\vec{r}) a_j(\vec{r} - \vec{n}) d\vec{r}. \quad (10)$$

Thus the partitioning of the DOS into contributions from even and odd symmetries is given by (8) to order k_y . We have tested our procedure by computing DOS with boxes of half the dimension shown in Fig. 4 and have obtained virtually identical results. This suggests that the error introduced by ignoring the opposite parity component of $\phi_j(\vec{k}_{\parallel}, \vec{r})$ is small.

In combination with the even and odd projections we may also project planar DOS by selecting only $a_j(\vec{r})$ belonging to a specific plane. We have elected to compute \vec{k}_{\parallel} -selected DOS for the central plane, surface plane, and the full slab as representative of the bulk, surface, and a surface-weighted average. The \vec{k}_{\parallel} -selected DOS along $\bar{\Gamma} - \bar{X}$ are presented in Figs. 5-7 and along $\bar{\Gamma} - \bar{M}$ in Figs. 8-10. The DOS have been folded with a Gaussian with a full width half maximum of 0.5 eV in line with expected experimental resolution, and in an attempt to minimize structure which is an artifact of the slab's having only 7 layers. We have tried to gauge the seriousness of this finite slab effect by comparing \vec{k}_{\parallel} -selected DOS for 7 and 9 planes of Cu(100). Our conclusion is that finite slab effects are perceptible, particularly in the low-density s -band regions of Cu, but are much smaller than, and do not mask, the real DOS structure.

The \vec{k}_{\parallel} -selected DOS may be generally characterized as having considerable structure which is strongly \vec{k}_{\parallel} dependent. The extent to which this

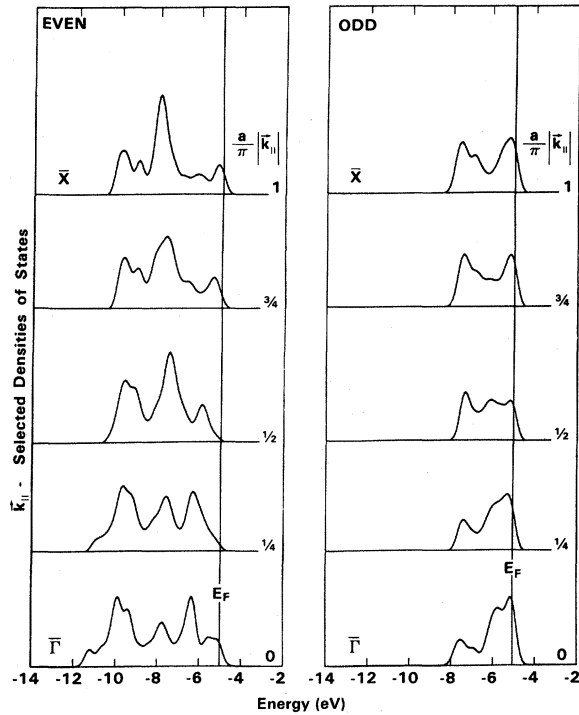


FIG. 5. \vec{k}_{\parallel} -selected densities of states for Pd(100) seven-layer film along $\bar{\Gamma}-\bar{X}$ [(110) azimuth].

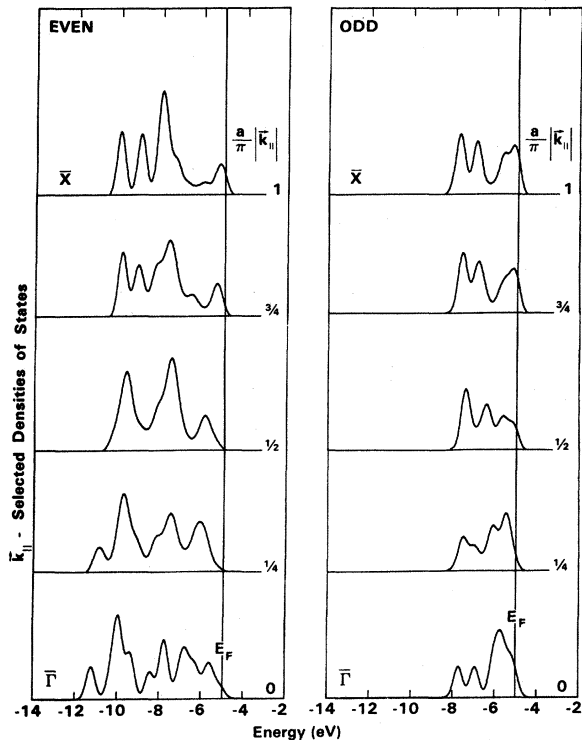


FIG. 6. \vec{k}_{\parallel} -selected densities of states for Pd(100) central plane along $\bar{\Gamma}-\bar{X}$ [(110) azimuth].

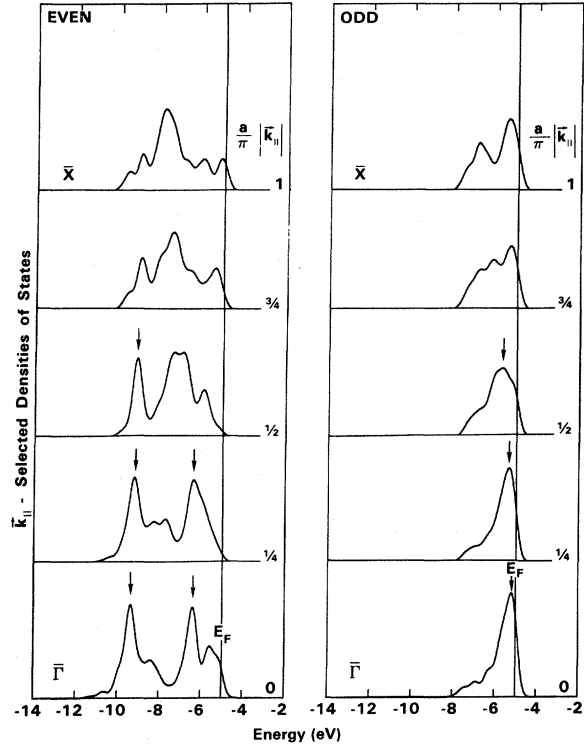


FIG. 7. \vec{k}_{\parallel} -selected densities of states for Pd(100) surface plane along $\bar{\Gamma}-\bar{X}$ [(110) azimuth]. The arrows indicate peaks which either are much larger in the surface than in the central plane or which exist only in the surface plane.

initial-state structure will be visible in angle-resolved photoemission experiments depends on the strength of matrix element and final-state effects. These effects diminish with increasing photon energy so that increasing correlation of spectra with the initial-state DOS is expected with higher photon energies. Note in each DOS figure that the even and odd results are qualitatively different. This indicates the importance of using polarized light in photoemission. With unpolarized light there is some unknown weighting of these even and odd distributions. This to our knowledge is the first investigation of the variation with \vec{k}_{\parallel} and mirror plane symmetry of the density of states. For each \vec{k}_{\parallel} region one may compute the area under the even and the area under the odd DOS and compute the even fraction. For a filled d band this fraction would be 0.60 for each \vec{k}_{\parallel} , but may be larger or smaller for an unfilled hybridized spd band. For the DOS of Figs. 5–10 we find fractions ranging from 0.60 to 0.76 indicating that the filled states are preponderantly even.

Figures 6, 7, 9, and 10 show that there are similarities between the central-plane results, which are representative of the bulk, and the sur-

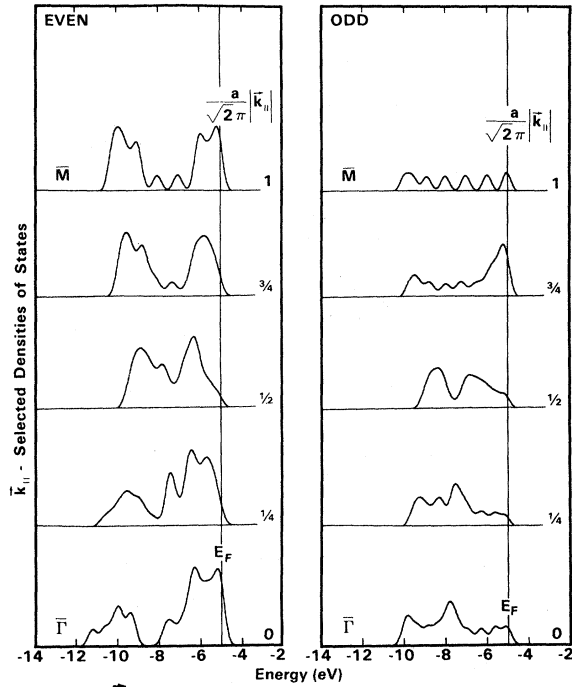


FIG. 8. \vec{k}_{\parallel} -selected densities of states for Pd(100) seven-layer film along $\bar{\Gamma}-\bar{M}$ [(100) azimuth].

face-plane results. There are also marked differences which are primarily due to surface states. In Figs. 7 and 10 we have noted with arrows peaks in the surface-plane DOS which are much smaller

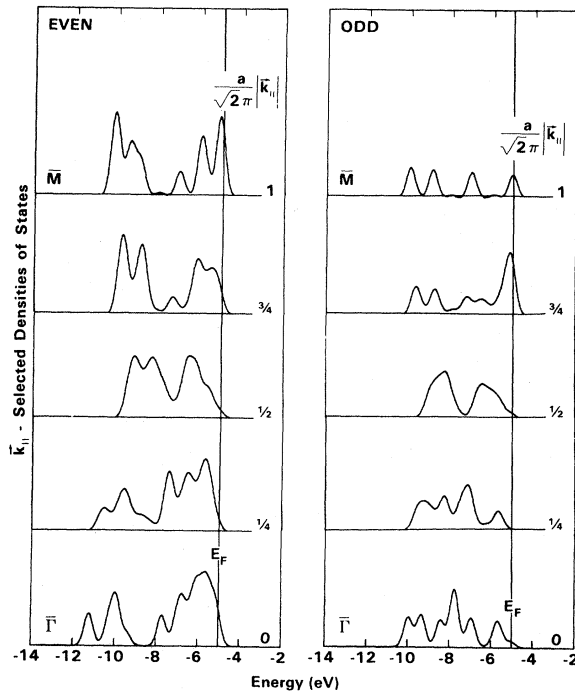


FIG. 9. \vec{k}_{\parallel} -selected densities of states for Pd(100) central plane along $\bar{\Gamma}-\bar{M}$ [(100) azimuth].

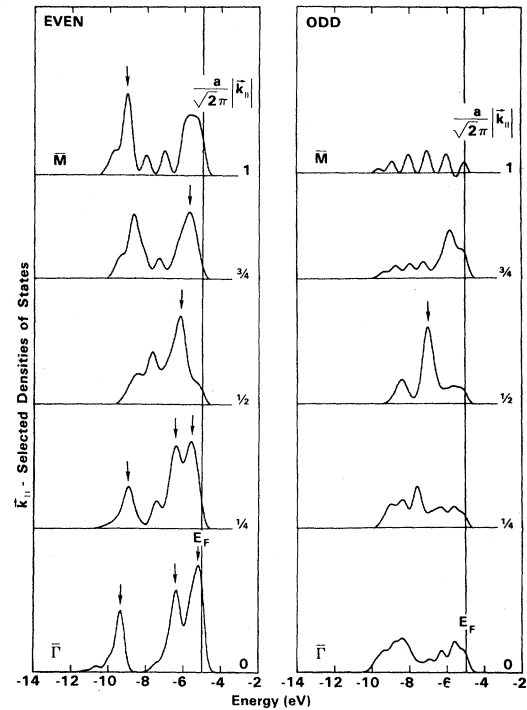


FIG. 10. \vec{k}_{\parallel} -selected densities of states for Pd(100) surface plane along $\bar{\Gamma}-\bar{M}$ [(100) azimuth]. The arrows indicate peaks which are either much larger in the surface than in the central plane or which exist only in the surface plane.

in the central plane or are not present at all.

One may correlate features observed in \vec{k}_{\parallel} -selected DOS with the band structure of Fig. 2. In Fig. 11 we have reproduced the portion of the $\bar{\Gamma}-\bar{M}$ panel of Fig. 2 lying below E_F . The states along each vertical line at 0, $\frac{1}{4}$, $\frac{1}{2}$, $\frac{3}{4}$, and 1 correspond to the respective plots in Figs. 8, 9, and 10. Note the low-density region between -6 and -9 eV at \bar{M} which is also clearly visible in the DOS plots. Another correspondence, for example, is found in the three even peaks at $\bar{\Gamma}$ marked as surface-state peaks in Fig. 10. These clearly correspond to the surface state bands at -9 , -6.5 , and -5 eV at $\bar{\Gamma}$ in Fig. 11. It is hoped that identifying surface-state features in the DOS as is done in Figs. 7 and 10 will help experimentalists isolate surface-state bands. Once candidate peaks are observed in the appropriate energy and momentum range, they may be checked for being surface features by varying the photon energy and making certain these peaks do not disperse with k_{\perp} .

The only angle-resolved experiments on Pd(100) are for normal emission¹² at 16.8 and 21.2 eV. The photon beam is not polarized so we are not able to determine which of our spectra at $\bar{\Gamma}$ should be compared with their data. The spectra are

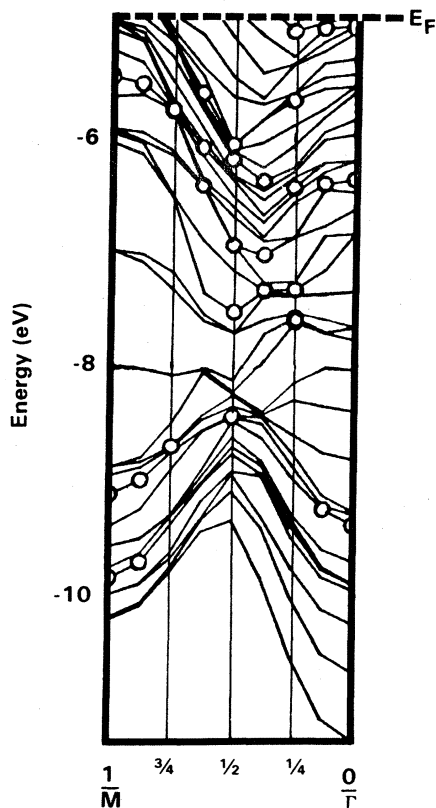


FIG. 11. Surface band structure along $\bar{\Gamma}-\bar{M}$.

much different at the two energies in any case. The authors attribute this to matrix element effects.

IV. SUMMARY

It has been found that 19% of the electrons in the surface layer of Pd(100) are in surface states. This is to be compared with the 23% found for Ni(100) and the 36% found for Cu(100). One would have to conclude from these studies that surface states must be considered in all future analyses of transition-metal surface electronic structure.

The results were analyzed in a new way by computing \vec{k}_{\parallel} -selected densities of states. We found that the densities of states varied quite rapidly with \vec{k}_{\parallel} and with mirror plane symmetry. The surface results were often quite different from those of the central plane. While surface-state bands are difficult to find experimentally on metal surfaces, the identification of surface-state peaks in \vec{k}_{\parallel} -selected densities of states may be helpful in locating them experimentally.

Note added in proof. A calculation of the electronic structure of silver (100) was carried out subsequent to the palladium calculation discussed in this paper. A paper covering that calculation has appeared in Phys. Rev. B 22, 4757 (1980). For silver (100), 22% of the surface layer electrons are in surface states.

- ¹J. R. Smith, J. G. Gay, and F. J. Arlinghaus, Phys. Rev. B **21**, 2201 (1980). See also *Theory of Chemisorption*, Vol. 19 of *Topics in Current Physics*, edited by J. R. Smith (Springer, New York, 1980), Chap. 4.
- ²J. G. Gay, J. R. Smith, and F. J. Arlinghaus, Phys. Rev. Lett. **42**, 332 (1979).
- ³F. J. Arlinghaus, J. G. Gay, and J. R. Smith, Phys. Rev. B **21**, 2055 (1980).
- ⁴Gary G. Tibbetts, James M. Burkstrand, and J. Charles Tracy, Phys. Rev. B **15**, 3652 (1977).
- ⁵D. T. Ling, J. N. Miller, P. A. Pianetta, D. L. Weissman, I. Lindau, and W. E. Spicer, J. Vac. Sci. Technol. **15**, 495 (1978).
- ⁶P. Heimann, J. Hermanson, H. Miosga, and H. Neddermeyer, Phys. Rev. B **20**, 3059 (1979). See also S. D. Kevan and D. A. Shirley, Phys. Rev. B **22**, 542 (1980), and D. Westphal and A. Goldmann, Surf. Sci. **95**, L249 (1980).
- ⁷K. S. Bohn, D. G. Dempsey, Leonard Kleinman, and Ed Caruthers, Phys. Rev. B **13**, 1515 (1976).
- ⁸C. M. Bertoni, O. Bisi, C. Calandra, F. Nizzoli, and G. Santors, J. Phys. F **6**, L41 (1976).
- ⁹D. G. Dempsey and Leonard Kleinman, Phys. Rev. B **16**, 5356 (1977).
- ¹⁰S. G. Louie, Phys. Rev. Lett. **40**, 1525 (1978).
- ¹¹J. E. Demuth, Surf. Sci. **65**, 369 (1977).
- ¹²D. R. Lloyd, C. M. Quinn, and N. V. Richardson, Surf. Sci. **63**, 174 (1977).
- ¹³V. L. Moruzzi, J. F. Janak, and A. R. Williams, *Calculated Electronic Properties of Metals* (Pergamon, New York, 1978), p. 145.
- ¹⁴K. Horn, N. V. Richardson, A. M. Bradshaw, and J. K. Sass, Solid State Commun. **32**, 16 (1979).
- ¹⁵A. M. Bradshaw, private communication.
- ¹⁶R. Podloucky, R. Lässen, E. Wimmer, and P. Weinberger, Phys. Rev. B **19**, 4999 (1979).
- ¹⁷G. D. Mahan, Phys. Rev. B **2**, 4334 (1970).
- ¹⁸W. L. Schaich and N. W. Ashcroft, Phys. Rev. B **3**, 2452 (1971).
- ¹⁹N. V. Smith, Phys. Rev. B **9**, 1365 (1974).
- ²⁰P. J. Feibelman and D. E. Eastman, Phys. Rev. B **10**, 4932 (1974).
- ²¹L. F. Wagner, Z. Hussain, and C. S. Fadley, Solid State Commun. **21**, 257 (1977).
- ²²N. J. Shevchik and D. Liebowitz, Phys. Rev. B **16**, 2395 (1977).
- ²³M. Sagurton and N. J. Shevchik, Phys. Rev. B **17**, 3859 (1978).
- ²⁴See P. Heimann, H. Neddermeyer, and H. F. Roloff, Phys. Rev. Lett. **37**, 775 (1976), and references therein. See also J. Stohr, P. S. Wehner, R. S. Williams, G. Apai, and D. A. Shirley, Phys. Rev. B **17**, 987 (1978).
- ²⁵J. Hermanson, Solid State Commun. **22**, 9 (1977).